

## Formation and performance of new Zr-Ti-Cu-Ni-Be-Fe bulk amorphous alloy

ZHAO Deqian (赵德乾)<sup>1</sup>, WANG Weihua (汪卫华)<sup>1</sup>,  
ZHUANG YANXIN (庄艳歆)<sup>1</sup>, PAN Mingxiang (潘明祥)<sup>1</sup>,  
JI Yingfei (季颖斐)<sup>2</sup>, MA Xueming (马学鸣)<sup>2</sup> & DONG Yuanda (董远达)<sup>2</sup>

1. Institute of Physics, Chinese Academy of Sciences, Beijing 100080, China;

2. Institute of Material, Shanghai University, Shanghai 200072, China

Correspondence should be addressed to Zhao Deqian (email: zhaodq@aphy.iphy.ac.cn)

Received July 28, 1999

**Abstract** The formation of the new Zr-Ti-Cu-Ni-Be-Fe bulk amorphous alloy with high strength is reported. The effects of the iron atom on the glass forming ability, hardness, susceptibility and thermal stability of the amorphous alloy are investigated. The role of the iron in the formation of the bulk amorphous alloy is discussed.

**Keywords:** bulk amorphous alloy, glass forming ability, Zr-Ti-Cu-Ni-Be-Fe alloy, hardness, susceptibility.

Recently, a series of multicomponent bulk amorphous alloys (e.g. Zr-Ti-Cu-Ni-Be amorphous alloy) consisting of common metals or nonmetals have been successfully developed. The critical cooling rates for the glass formation are less than 10 K/s, which are much lower than those of the traditional amorphous alloys, and their glass forming ability (GFA) is close to that of the oxide glasses. These amorphous alloys can be made into rods with the largest cross-section of 50 mm, with simple technique and low cost and excellent properties (e.g. high strength, good corrosion resistance and ductility). These amorphous alloys exhibit a high thermal stability and a large supercooled liquid region (between 30 and 100 K). In the supercooled liquid state, the liquid structure of the alloy keeps almost unchanged, while the viscosity of the alloy is close to that of the solid state, so these alloys provide us ideal materials to study the physical properties and structures of the supercooled liquids. The novel amorphous alloys are believed to have considerable importance in science and technology, and have aroused great interest<sup>[1,2]</sup>.  $Zr_{41}Ti_{14}Cu_{12.5}Ni_{10}Be_{22.5}$  is of the best GFA known so far, whose minimum critical cooling rate for glass formation is about 1 K/s<sup>[3]</sup>. The amorphous alloy is of excellent mechanical and physical properties. In this work, the formation of new Zr-Ti-Cu-Ni-Be-Fe amorphous alloy with high thermal stability and strength by means of replacing nickel atom with iron is reported. Anomalous changes of susceptibility of the alloys nearby the crystallization temperature have been observed. The effects of the iron atom on the glass forming ability and the formation mechanism of the amorphous alloy are discussed.

### 1 Experiment

99.99% and 99.999% pure Zr, Ti, Cu, Ni, Be and Fe were melted together by arc furnace under a Ti-gettered Ar atmosphere to form homogeneous alloy ingots of desired compositions.

The ingots were remelted together in a silica tube with  $10^{-3}$  Pa vacuum and subsequently quenched in water to form cylindrical rods with diameter 8—16 mm and length 100—200 mm. The nominal components are  $Zr_{41}Ti_{14}Cu_{12.5}Ni_{10-x}Be_{22.5}Fe_x$  (atomic percent,  $x = 0, 2, 5, 10$ ). The sample was weighed at various stages in the alloying process to check the loss of the product. The weight loss of the samples after melting was less than 0.1%; thus the composition of the alloys did not change significantly after melting. The sample rods were cut transversely, and the cross-sectional slices were investigated by X-ray diffraction (XRD), differential scanning calorimetry (DSC), microhardness and susceptibility test. XRD was performed on a Siemens D5000 diffractometer with  $CuK\alpha$  radiation. DSC was carried out with a calibrated high-temperature calorimeter of the Perkin Elmer DTA-7 type under pure flowing Argon gas.  $H_v$  of the alloy was obtained by a metallographical microscope of the Neophot-21 type attached microhardness meter, and experimental results were Vickers hardness. Susceptibility was performed on a model MB-2 magnetic balance, with magnetic field intensity of 1.2 T and magnetic gradient of  $1.3 \times 10^7$  Oe<sup>2</sup>/cm.

## 2 Results and discussion

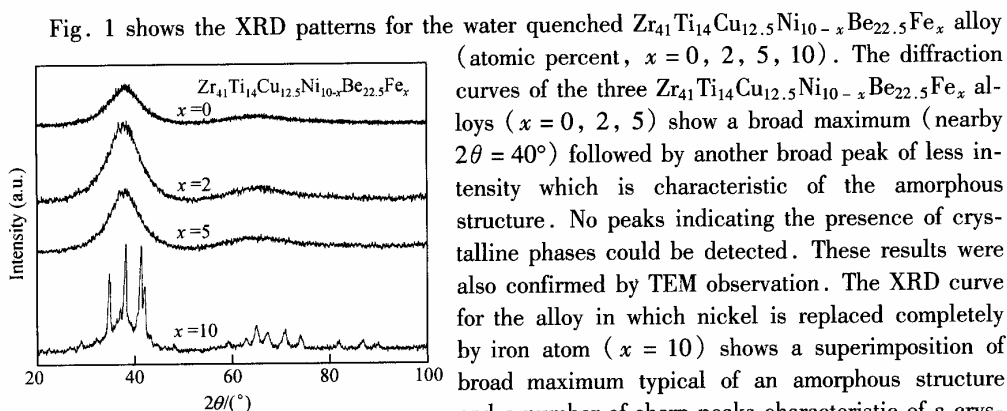


Fig. 1. X-ray diffraction patterns for the water quenched  $Zr_{41}Ti_{14}Cu_{12.5}Ni_{10-x}Be_{22.5}Fe_x$  ( $x = 0, 2, 5, 10$ ).

Fig. 1 shows the XRD patterns for the water quenched  $Zr_{41}Ti_{14}Cu_{12.5}Ni_{10-x}Be_{22.5}Fe_x$  alloy (atomic percent,  $x = 0, 2, 5, 10$ ). The diffraction curves of the three  $Zr_{41}Ti_{14}Cu_{12.5}Ni_{10-x}Be_{22.5}Fe_x$  alloys ( $x = 0, 2, 5$ ) show a broad maximum (nearby  $2\theta = 40^\circ$ ) followed by another broad peak of less intensity which is characteristic of the amorphous structure. No peaks indicating the presence of crystalline phases could be detected. These results were also confirmed by TEM observation. The XRD curve for the alloy in which nickel is replaced completely by iron atom ( $x = 10$ ) shows a superimposition of broad maximum typical of an amorphous structure and a number of sharp peaks characteristic of a crystalline phase, suggesting the presence of a mixture of amorphous and crystalline phases in this alloy.

When other elements were replaced by iron atom, the GFA of the alloy is reduced greatly, and bulk amorphous alloy cannot be obtained.

Fig. 2 shows a comparison of DSC traces for the amorphous  $Zr_{41}Ti_{14}Cu_{12.5}Ni_{10-x}Be_{22.5}Fe_x$  alloy ( $x = 0, 2, 5, 10$ ). Their heating rate is 10 K/min. Fig. 2(a) and 2(b) are DSC traces of the crystallization peaks and melting peaks for amorphous  $Zr_{41}Ti_{14}Cu_{12.5}Ni_{10-x}Be_{22.5}Fe_x$  alloys respectively. The first crystallization temperatures  $T_{x1}$ , crystallization enthalpy  $\Delta H_x$ , melting enthalpy  $\Delta H_m$ , glass transition temperatures  $T_g$  and melting temperatures  $T_m$  are listed in table 1. For the  $Zr_{41}Ti_{14}Cu_{12.5}Ni_{10}Be_{22.5}$  alloy,  $T_g$  is 645 K, and  $T_{x1}$  is 706 K.  $\Delta T = T_{x1} - T_g$  for the supercooled liquid region is 61 K.  $T_g$ ,  $T_{x1}$  and  $\Delta T$  of the  $Zr_{41}Ti_{14}Cu_{12.5}Ni_{10-x}Be_{22.5}Fe_x$  alloys are shown in fig. 2(a) and table 1.  $T_g$  is almost the same as that of the alloy without iron addition. However, the added iron decreases  $T_{x1}$  about 30 K, and decreases the supercooled liquid region. As shown in the DSC curves, the shape and number of peaks of four DSC curves are also different, meaning that the crystallization products are changed by iron addition. The crystallization

enthalpy of alloys is increased for the alloy with  $x = 2$  at. %, and then reduced from 118.25 J/g to 68.39 J/g with increasing iron content. Comparing with  $Zr_{41}Ti_{14}Cu_{12.5}Ni_{10}Be_{22.5}$  alloy, the crystallization enthalpy of alloys is reduced from 109.03 J/g to 68.39 J/g. As shown in table 1 and fig. 2(b),  $T_m$  of alloys is increased about 34 K with increasing Fe content.

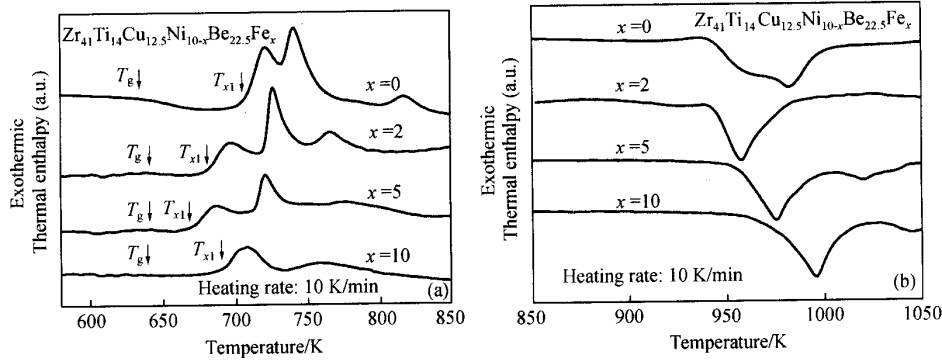


Fig. 2. DSC traces of the bulk amorphous alloys  $Zr_{41}Ti_{14}Cu_{12.5}Ni_{10-x}Be_{22.5}Fe_x$ . (a) DSC trace of crystalline peaks; (b) DSC trace of melt peaks.

Table 1  $T_x$ ,  $T_g$ ,  $T_m$ ,  $\Delta H_x$  and  $\Delta H_m$  of the  $Zr_{41}Ti_{14}Cu_{12.5}Ni_{10-x}Be_{22.5}Fe_x$  alloy

Samples	$T_g/K$	$T_{x1}/K$	$\Delta T/K$	$\Delta H_x/J \cdot g^{-1}$	$T_m/K$	$\Delta H_m/J \cdot g^{-1}$
$x = 0$	645	706	61	-109.03	941	125.33
$x = 2$	644	680	36	-118.25	941	144.79
$x = 5$	639	669	30	-116.18	954	146.48
$x = 10$	638	690	52	-68.39	975	159.12

Fig. 3 shows the effects of the Fe addition on the Vickers hardness ( $H_V$ ) of the alloys. The  $H_V$  of the alloy without Fe is 5.4 GPa. The  $H_V$  of the alloys is increased from 5.4 GPa to 8.99 GPa and 6.82 GPa by 2 at. % Fe and 5 at. % Fe addition. But the  $H_V$  of the alloys is reduced with more Fe addition. The  $H_V$  of the alloy with 10 at. % Fe addition is reduced to 4.38 GPa. These results show that the strength of the bulk amorphous alloy can be enhanced greatly by iron addition properly.

Fig. 4 shows the susceptibility dependence of temperature for the bulk amorphous  $Zr_{41}Ti_{14}Cu_{12.5}Ni_{10-x}Be_{22.5}Fe_x$  alloy. Since  $T_x$  is related to the heating rate, 10 K/min was adopted to accord with that of

DSC test. As shown in fig. 4, the susceptibility  $\chi$  of the amorphous alloy with 5 at. % Fe addition shows a sudden change nearby  $T_x$ . Fig. 5 shows temperature dependence of the susceptibility for alloys. The susceptibility of the alloys is positive, indicating that the alloys are still paramagnetism after iron addition. The susceptibility of the Fe added amorphous alloys has significant change near  $T_g$  and  $T_x$ . The abnormal phenomena are similar to the changes of susceptibility at

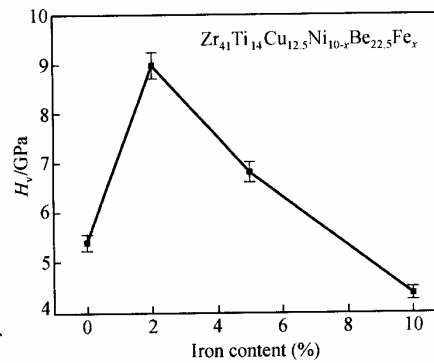


Fig. 3. The effect of the iron concentration on the Vickers hardness ( $H_V$ ).

melting temperature in some metals<sup>[4]</sup>. The relatively slow change of susceptibility of amorphous  $Zr_{41}Ti_{14}Cu_{12.5}Ni_{10}Be_{22.5}$  alloy has also been observed near  $T_x$ . Farther research work is needed to understand the abnormal phenomena.

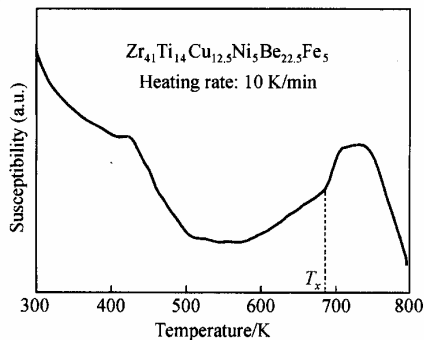


Fig. 4. The susceptibility dependence of temperature for the amorphous alloy  $Zr_{41}Ti_{14}Cu_{12.5}Ni_5Be_{22.5}Fe_5$ .

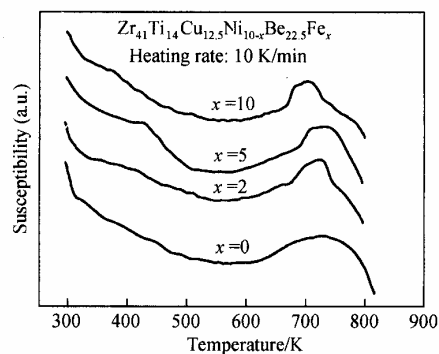


Fig. 5. The susceptibility dependence of temperature for the amorphous alloys  $Zr_{41}Ti_{14}Cu_{12.5}Ni_{10-x}Be_{22.5}Fe_x$ .

Zr-Ti-Cu-Ni-Be is of the best GFA known so far. By substituting Ni with Fe properly, the bulk amorphous alloys with good GFA can be also obtained with high thermal stability. The critical cooling rates of these alloys are less than 10 K/s. Their diameters are from 8 mm to 16 mm. These results indicate that Zr-Ti-Cu-Ni-Be-Fe alloys have excellent GFA. The mechanism for the excellent glass forming alloy can be discussed in structural, thermodynamic and kinetic aspects. In structural aspect, Fe atomic radius is close to that of Ni, there are significant differences in atomic size among the six constituent elements of the alloy. The studies on microstructures indicate that the multicomponent amorphous alloy has random closer packing structure than that of the binary amorphous alloys<sup>[5]</sup>. This kind of microstructure, resulting from the significant atomic size differences among the constituent elements, suppresses nucleation and growth of the crystalline phase in the supercooled liquid state by inhibiting the long distance diffusion and increasing the melting viscosity. In thermodynamics, Fe proper addition results in relatively low eutectic melting temperature of the alloy ( $T_m < 800^\circ\text{C}$ ), and the reduced glass transition temperature  $T_{rg}$  ( $T_{rg} = T_g/T_m$ ) is larger than 0.65. The larger the  $T_{rg}$ , the stronger the glass forming ability. The multicomponent bulk amorphous alloy has highly random close packing microstructure, and its composition and local microstructure are much different from those of the crystallization phases<sup>[6]</sup>. The local atomic configuration of short range order and composition in the conventional amorphous alloys resemble the corresponding equilibrium compounds with compositions near those of the amorphous alloys (for example,  $MgZn_2$  Laves phase)<sup>[7]</sup>. The crystallization process occurs easily because it does not need long range diffusion of the atoms, so high cooling rate is needed for suppressing nucleation and growth of the crystalline phase. The microstructural characteristics of the new bulk amorphous alloy make the component elements substantial redistribution. On the other hand, the highly random close packing structure and large viscosity make the redistribution of atoms on a large range scale extremely difficult. The more the components, the more difficult for all constituents to simultaneously satisfy the local structural and compositional requirements of the crystalline phases. This argument is called "confusion principle"<sup>[8]</sup>. Kinetically, the multicom-

ponents and the microstructural characteristics lead to an excellent GFA and high thermal stability of the Zr-Ti-Cu-Ni-Be-Fe alloy.

### 3 Conclusions

1) Bulk amorphous alloys with high thermal stability, excellent GFA and higher hardness are developed.

2) The anomalous temperature-dependent change of susceptibility is observed nearby crystallization temperature of bulk amorphous Zr-Ti-Cu-Ni-Be-Fe alloys.

**Acknowledgements** This work was supported by the National Natural Science Foundation of China (Grant No.59871059) and Spaceflight High Technology (863-2) Youth Science Foundation.

### References

1. Inoue, A., High strength bulk amorphous alloys with low critical cooling rates, *Mater. Trans. JIM*, 1995, 36: 866.
2. Johnson, W. L., Fundamental aspects of bulk metallic glass formation in multicomponent alloy, *Mater. Sci. Forum*, 1996, 35: 225.
3. Peker, A., Johnson, W. L., A highly processable metallic glass:  $Zr_{41}Ti_{14}Cu_{12.5}Ni_{10}Be_{22.5}$ , *Appl. Phys. Lett.*, 1993, 63: 2342.
4. Dai Daosheng, Qian Kunming, *Ferromagnetics*, Beijing: Science Press, 1992, 28—315.
5. Wang, R., Short range structure for amorphous intertransition metal alloy, *Nature*, 1979, 278: 700.
6. Wang, W. H., Wei, Q., Wollenberger, H. et al., Microstructure, decomposition, and crystallization in  $Zr_{41}Ti_{14}Cu_{12.5}Ni_{10}Be_{22.5}$  bulk metallic glass, *Phys. Rev. B*, 1998, 57: 8211.
7. Wang, W. H., Wei, Q., Wollenberger, H. et al., Microstructure studies of  $Zr_{41}Ti_{14}Cu_{12.5}Ni_{10}Be_{22.5}$  amorphous alloy by electron diffraction intensity analysis, *Appl. Phys. Lett.*, 1997, 71: 1053.
8. Greer, A. L., Confusion by design, *Nature*, 1993, 366: 303.